Research Paper

Elucidation of the anti-colorectal cancer mechanism of *Atractylodes lancea* by network pharmacology and experimental verification

Guangliang Wang[1,2,*], Chuangchuang Guo[3,*], Hui Pi[4,*], Yu Wang[1], Shuyun Lin[1], Keyi Bi[5], Ming Zhang[1], Na Wang[3], Guojun Zhao[1]

[1]Affiliated Qingyuan Hospital (Qingyuan People's Hospital), Guangzhou Medical University, Qingyuan 511518, Guangdong, China
[2]Department of Histology and Embryology, Faculty of Basic Medical Sciences, Guilin Medical University, Guilin 541000, Guangxi, China
[3]Faculty of Public Health, Guilin Medical University, Guilin 541000, Guangxi, China
[4]Faculty of Basic Medical Sciences, Dali University, Dali 671003, Yunnan, China
[5]Department of Pharmacy, Guilin Medical University, Guilin 541000, Guangxi, China
*Equal contribution

Correspondence to: Na Wang, Guojun Zhao; **email:** wnhb2016@163.com, https://orcid.org/0000-0001-6798-7266; zhaoguojun@gzhmu.edu.cn
Keywords: colorectal cancer, *Atractylodes lancea*, network pharmacology, molecular docking, luteolin
Received: December 4, 2023 **Accepted:** July 13, 2024 **Published:** August 22, 2024

ABSTRACT

Atractylodes lancea **which was listed in "Shennong's Materia Medica" and could be used to treat gastrointestinal-associated diseases. However, its roles, core and active ingredients, and mechanisms in treatment of colorectal cancer (CRC) were still unknown. Therefore, network pharmacology and experimental validation were used to clarify the effects, core active ingredients and molecular mechanisms of** ***Atractylodes lancea*****. We found that** ***Atractylodes lancea*** **has 28 effective active components and 213 potential targets. Seventy-three genes which demonstrate interaction between the** ***Atractylodes lancea*** **and CRC were confirmed. Enrichment analysis showed that 2033 GO biological process items and 144 KEGG pathways. Survival and molecular docking analysis revealed that luteolin as the core component interacted with these genes (Matrix metalloproteinase 3 (MMP3), Matrix metalloproteinase 9 (MMP9), Tissue inhibitor of metalloproteinases 1 (TIMP1), Vascular endothelial growth factor A (VEGFA)) with the lowest binding energy, and these genes were involved in building a prognostic model for CRC. Cellular phenotyping experiments showed that luteolin could inhibit the proliferation and migration of CRC cells and downregulate the expression of MMP3, MMP9, TIMP1, VEGFA probably by Phosphoinositide 3-kinase/ serine/threonine kinase Akt (PI3K/AKT) pathway. To conclude,** ***Atractylodes lancea*** **could inhibit proliferation and migration of CRC cells through its core active ingredient (luteolin) to suppress the expression of MMP3, MMP9, TIMP1, VEGFA probably by PI3K/AKT pathway.**

INTRODUCTION

Colorectal cancer (CRC) is one of the most commonly diagnosed digestive cancers in the world. About 60-70% of CRC patients were diagnosed at the late stage [1]. 25%-30% of patients present with metastases [2]. A series of factors that lead to the development of CRC include obesity, smoking and eating red meat [3]. At present, the methods treatment for CRC is still surgery, supplemented by chemotherapy and radiotherapy [4]. Currently, traditional chemotherapeutic drugs inhibit and kill no matter of tumor cells, but normal cells, moreover, due to the effects of toxic side and drugs resistance of tumor, many drugs are limited to clinical applications [4].

Therefore, it was necessary to discover new drugs to achieve the high efficiency anti-tumor ability with low toxicity. In traditional Chinese medicine, some plants with the characteristics of low-toxicity anti-tumor properties. This study was aimed to provide theoretical support to develop these low toxicity, plant-based drugs.

Phytochemicals, as natural substances in plants, are important resources for the development of novel anti-tumor drugs. Research and clinical studies assume that phytochemicals have anti-carcinogenic effects, including inhibiting proliferation, inducing apoptosis, and enhancing the excretion of carcinogens [5]. *Atractylodes lancea* (Chinese: Cangzhu) was a widely used traditional Chinese medicine (TCM) and listed in "Shennong's Materia Medica", the rhizome tastes pungent and bitter, and was attributed to the spleen, stomach and liver meridians. According to the theory of TCM, *Atractylodes lancea* could be used to treat rheumatic diseases, digestive disorders, night blindness, and influenza. *Atractylodes lancea* was generally used in Ermiao Powder, Simiao Powder and so on in traditional decoctions. Recently, it was found that *Atractylodes lancea* extracts also have anti-cancer and anti-inflammatory effects [6]. Additionally, recent studies have shown that *Atractylodes lancea* could inhibit proliferation by cellular signaling pathways involved in gastric cancer cells [7], Cholangiocarcinoma (CCA) [8], non-small cell lung cancer [9] and so on. Among these researches, it has been reported the ethanolic extract of *Atractylodes lancea* inhibits the progress of Opisthorchis viverrini/dimethyl-nitrosamine (DMN)-induced CCA model and CCA-xenografted nude mice without significant toxicity, compared with 5-FU and the untreated control [10, 11]; phase I and II clinical trial have shown that it can improve clinical response and disease progression of CCA patients [12, 13]. In CRC studies, as adjunctive therapy, *Atractylodes lancea* could relieve nausea, vomiting and neutropenia after Oxaliplatin treatment [14, 15]; mixtures consisting of *Atractylodes lancea* were significantly inhibited metastasis of CRC in murine lung-metastasis model [16]; 13 randomized controlled trials were analyzed and found that *Atractylodes lancea* could have contributed to improve CRC response [17]. However, the role, core active ingredients and mechanism of *Atractylodes lancea* in the treatment of CRC are currently less studied.

In drug development, developing multi-targeted drugs for complex diseases such as cancer was rapidly growing. Network pharmacology could systematically observe the impact of drugs on diseases, thereby revealing the complexity of Chinese medicine and disease through the interaction of "disease-gene-protein-drug" [18]. Studies have shown that network pharmacology has been used to reveal the potential activity of ingredients, targets and mechanisms of Chinese medicine in the treatment of disease, and to provide new strategies to develop new drugs [19]. In this study, we found that luteolin as the core active component of *Atractylodes lancea* plays an anti-CRC role and its molecular mechanism against CRC by network pharmacology and experimental verification.

MATERIALS AND METHODS

Target collection for *Atractylodes lancea*

Pharmacological platforms such as HIT [20], TCMSP [21] and TCMID [22] were utilized to search for the active components of *Atractylodes lancea*. The results of the search were combined to remove the compounds that were duplicate and did not have PubChem ID. According to the PubChem ID, the target gene corresponding to the active ingredient was retrieved in HIT.

Identify critical genes for CRC from disease databases

Using "colorectal cancer" and "colorectal adenoma" as search terms, we searched the GeneCards [23], OMIM [24] and DigSee [25] databases for potential targets which related to CRC. Targets from these three disease databases were combined and duplicate values were removed to obtain CRC related targets.

Identify key genes in CRC from expression data

We obtained expression data separately from Gene Expression Omnibus (GEO) and The Cancer Genome Atlas (TCGA) databases. GSE164191 was obtained from the GEO database (http://www.ncbi.nlm.nih.gov/geo/) and includes expression profiles of 59 CRC peripheral blood samples and 62 normal peripheral blood samples. Limma package [26] was used to check raw gene expression data. Volcano plots of CRC VS Normal were created to indicate significantly up- and down-regulated genes. Genes with adjusted p-value less than 0.05 were screened and considered as Differential Expression Genes (DEGs). The top 100 DEGs obtained from the above process were used for further studies. Heatmap of the dataset was plotted using SRplot (https://www.bioinformatics.com.cn/) and network of DEGs was plotted using Cytoscape.

PPI network construction

Targets obtained from disease database were integrated and Venn diagram [27] was plotted to identify genes shared by targets of *Atractylodes lancea* and CRC. Protein-protein interaction (PPI) networks were created using STRING [28] (http://string-db.org). Interaction

scores were set at 0.4 ~ 10. The hub genes and crucial modules of the *Atractylodes lancea* anti-CRC from PPI network were calculated using the MCC algorithm in the CytoHubba plug-in for CytoScape, and then the network of related protein targets was constructed. Finally, the top 10 core targets were also displayed.

Pathway and functional enrichment analysis

In order to clarify the roles of target proteins interacting with the target genes of *Atractylodes lancea* in gene functions and signaling pathways, we performed Gene Ontology (GO) and Kyoto Encyclopedia of Genes and Genomes (KEGG) enrichment analysis of potential targets of *Atractylodes macrocephala* for intervention in CRC using clusterProfiler [29]. The enriched GO terms and pathways with *p*-values less than 0.05 were selected for further visualization.

Correlation, expression and survival analysis

The correlation and expression among the hub genes were analyzed using Gene Expression Profiling Interactive Analysis (GEPIA). By multifactorial Cox regression analysis, the prognostic model constructed by the hub genes was able to accurately and efficiently classify CRC into different risk categories, and the survival of low-risk CRC patients was significantly longer than that of high-risk CRC patients. Meanwhile, the Area Under Curve (AUC) values for the prognostic model predicting 1-, 3-, and 5-year survival were determined by Receiver Operator Curves (ROC) curve analysis.

Molecular docking

The target genes corresponding to each active ingredient in the Chinese medicines were intersected with the intersection genes respectively, and the one with the most intersections was taken as the core ingredient of the drug. Molecular docking was performed in order to predict the interactions between these genes and *Atractylodes lancea* [30]. The structures of the target proteins were downloaded from the Protein Data Bank (PDB) database (https://www.rcsb.org). Water molecules and original ligands were removed from the protein structures using PyMOL. Proteins were further processed and docked using AutoDock Tools 1.5.6. Visualizations of the 3D interactions between the top four protein-*Atractylodes lancea* complexes with the lowest binding energies were built using PyMOL [31].

Cell culture

CRC cell lines NCM460, RKO, HCT15, SW480, SW620 and HT29 were purchased from Cell Bank of the Chinese Academy of Sciences (Shanghai, China), and were cultured in DMEM medium and RPMI1640 medium, respectively. All media supplement with 10% fetal bovine serum.

Cell viability assay

Collected log-phase cells, planted 2000 cells/well into 96-well and cultured. After incubation at 37° C for 24 h, the cells were treated with different concentrations of *Atractylodes lancea* at different times. Next, add 10 μL of Cell Counting Kit (CCK)-8 reagent to each well and continue incubation for 4 h. Then, the optical density (OD) values were measured at 450 nm with an enzyme meter.

EdU assay

Cells were cultured on coverslips and treated with 40 μM *Atractylodes lancea* for 24 h. Then cells were incubated with 5-ethynyl-2'-deoxyuridine (EdU) working solution for 2 h. Washed the cells with PBS, and incubated with stationary liquid for 30 min at room temperature, washed and permeabilizated (PBS containing 0.3% TritonX-100) for 10 min. After washing with PBS, click reaction solution was added and reacted for 1-2 hours away from light. Next, washed with PBS and added Hoechst 33,342 Reagent for 10 min. EdU-positive cells were measured under confocal microscopy.

Colony formation experiment

2000 cells/well were planted into 6-well with indicated treatment. Changed the medium and added drugs every two days. After 2 weeks, the colonies were clearly visible. Then the colonies were fixed with 4% paraformaldehyde, stained with crystal violet and photographed.

Wound-healing assay

When the density of cultured cells reached 90% confluence, a sterile pipette tip was used to produce wound. Cell culture medium was replaced with serum-free DMEM, and migration distance was observed and calculated using a microscope after 72 h.

RNA isolation and real-time PCR

TRlzol reagent was used to lysis to obtain total RNA according to manufacturer's instructions. Relevant mRNA expression levels were measured by qRT-PCR assay using SYBR Green PCR Master Mix (Takara, Japan, RR820A). The mRNA levels were normalized to 18s mRNA. Primer sequences were shown in Supplementary Table 1.

Western blot analysis

Lysis buffer was used to lyse cells, equal amounts of proteins were uploaded and electro-transferred to polyvinylidene fluoride (PVDF) membranes. 5% skim milk was used to block membranes for 2 h at room temperature and then primary antibodies (anti-MMP3 (AF0217, Affinity, USA, 1:2000), anti-MMP9 (AF5228, Affinity, 1:2000), anti-PI3K (A4992, Abclonal, USA 1:500), anti-p-PI3K (17366, CST, USA, 1:1000), anti-AKT (9272, CST, 1:1000), anti-p-AKT (4060, CST, 1:1000) or anti-GAPDH (5174, CST, 1:1000)) incubated membranes at 4° C overnight. Membranes were incubated with HRP-conjugated secondary antibody (1:1000, SeraCare, USA) for 2 h at room temperature and visualized using the Bio-Rad Image Detection System.

Statistical analysis

Data were analyzed using SPSS version 18.0. Data are presented as means ± standard deviation (SD) of at least three independent experiments. Normally distributed data sets were analyzed using an unpaired Student's t-test for two independent groups or a paired t-test for two dependent groups. *p*-values of < 0.05 were considered statistically significant, and *p*-values < 0.05, 0.01, and 0.001, were indicated by one, two, and three asterisks, respectively.

Data availability statement

The data supporting this study are available from the corresponding authors upon reasonable request.

RESULTS

Acquisition of the targets of *Atractylodes lancea*

The HIT, TCMSP and TCMID database were used to search for the core active ingredients of the *Atractylodes lancea*, 72 active ingredients were collected (Supplementary Table 2). According to the PubChem ID, the target genes which corresponding to active ingredients were searched in HIT, the active ingredient without target genes in the database was removed, and finally we got 213 target genes corresponding to 28 active ingredients (Supplementary Table 3).

Target screening for CRC

By searching the following databases: Genecards, OMIM, DigSee, 11535 genes related with CRC were collected (Supplementary Table 4). Considering the diagnostic and prognostic risk assessment, the peripheral blood datasets GSE164191 from CRC patients was utilized for analysis. 5239 upregulated and 3668 downregulated DEGs were obtained by applying the cut-off adj p-value < 0.05 to the datasets, respectively (Supplementary Table 5). And 6833 up-regulated and 8029 down-regulated genes were obtained in the same way (Supplementary Table 6). These DEGs in both data were used for volcano plots (Figure 1A, 1B), and the top 100 of them were displayed in heatmap (Figure 1C, 1D). The correlation between top 100 DEGs was visualized by using Cytoscape (Figures 1E, 1F).

Venn diagram and PPI network construction

The intersection of *Atractylodes lancea*-related target genes and CRC-related target genes was taken, and Venn map was drawn by VennDiagram (Version 1.7.3) to obtain 73 intersection targets (Figure 2A and Supplementary Table 7). Construction of relationship network for 73 genes and *Atractylodes lancea* active ingredients was done by using Cytoscape (Figure 2B).

The overlapped targets were submitted to STRING for PPI network construction, and the interacting proteins with a score cutoff > 0.4 and size cutoff < 10 were selected. Finally, 304 interaction relationships were collected and visualized by Cytoscape (Figure 3A). By using Cytohubba, the plug-in of Cytoscape, the hub genes were displayed in the interaction network. The top 10 hub genes of target proteins were identified, and a network was constructed. We found that STAT3, VEGFA, MMP9, IL6, HGF, TGFB1, MMP3, IL10, TIMP1, LBP were the important targets for *Atractylodes lancea* to intervene CRC (Figure 3B).

GO and KEGG analysis

To explore the possible mechanisms of the anti-CRC effect of *Atractylodes lancea*, 73 intersection targets were used to analysis GO and KEGG enrichment with R software and the results were visualized. GO enrichment analysis showed that a total of 2033 biological processes (BP) items, and the top 10 significantly enriched terms were displayed, according to $p < 0.05$ (Supplementary Table 8). The target proteins were involved in response to reactive oxygen species, response to oxidative stress, cellular response to chemical stress, cellular response to oxidative stress, regulation of apoptotic signaling pathway, epithelial cell proliferation, negative regulation of apoptotic signaling pathway, response to peptide, gland development, leukocyte proliferation (Figure 4A–4C). The top 10 significantly enriched terms of cellular components localization were primarily associated with extracellular space, Bcl-2 family protein complex, nucleoplasm, extracellular region, cytosol, endoplasmic reticulum, nucleus, mitochondrion, cytoplasm and macromolecular complex (Supplementary Figure 1A).

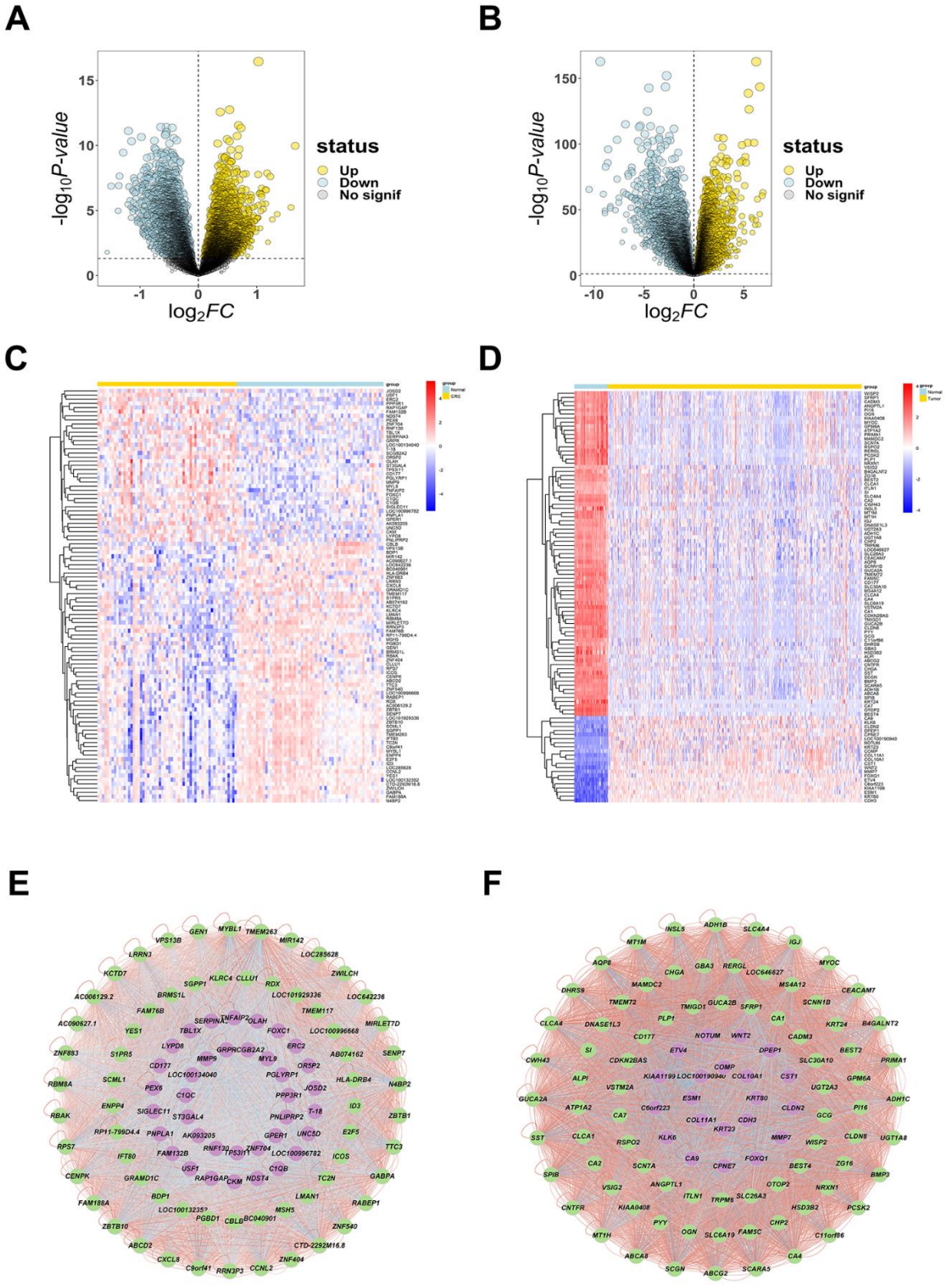

Figure 1. The DEGs of CRC. (**A**, **B**) The volcano plots were created to visualize differentially up- and down- regulated genes from GSE164191 and TCGA with significance p < 0.05, reseparate, up-regulated genes are shown in yellow color, down-regulated genes are shown in light blue color. (**C**, **D**) The heatmaps were to show the top 100 up- and down-expressed genes, up-regulated genes are shown in red color, down-regulated genes are shown in blue color. (**E**, **F**) Network diagram (arranged according to LogFC value) of top 100 DEGs were plotted to evaluate their correlation ship, up-regulated genes are shown in purple color, down-regulated genes are shown in green color, significant negative correlation ship are shown in blue lines, significant positive correlation ship are shown in red lines.

Additionally, the molecular function mainly involved identical protein binding, ubiquitin protein ligase binding, protein binding, protein kinase binding, RNA polymerase II sequence-specific DNA binding transcription factor binding, BH3 domain binding, protein homodimerization activity, cytokine activity, enzyme binding and trans-membrane receptor protein tyrosine kinase activity (Supplementary Figure 1B).There were 144 KEGG enrichment items in total, and the top 10 items were displayed according to p-values < 0.05 (Supplementary Table 9), included Hepatitis B, Prostate cancer, AGE-RAGE signaling pathway in diabetic complications,

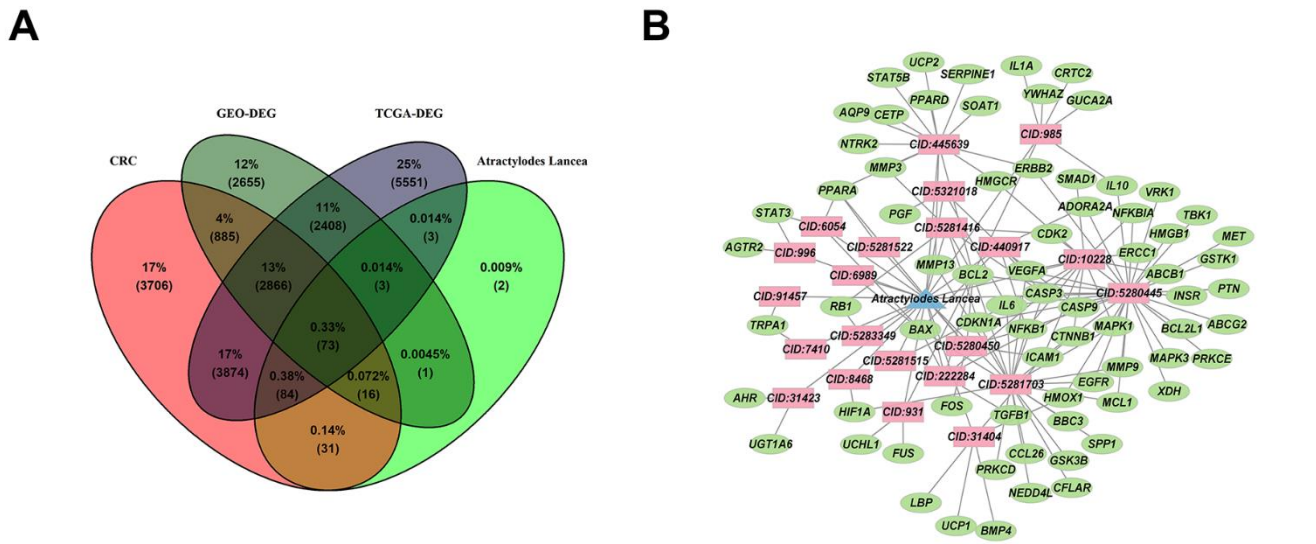

Figure 2. The targets and relationship between *Atractylodes lancea* and CRC. (**A**) The co-expression of 73 genes between targets of *Atractylodes lancea* and CRC were overlapped in Venn map. (**B**) Cytoscape constructs a network of relationships between 73 genes and active ingredients of *Atractylodes lancea*, active ingredients are shown in red color, *Atractylodes lancea* are shown in blue color, genes are shown in green color.

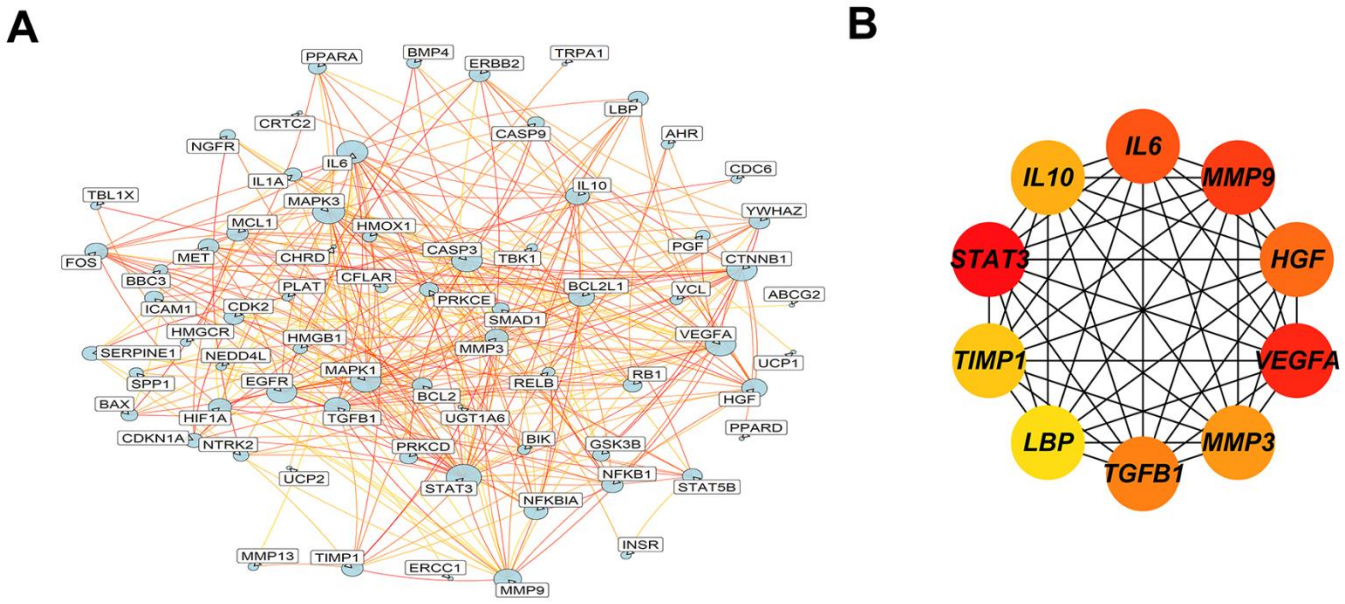

Figure 3. Protein–protein interaction network diagram of 73 intersected DEGs. (**A**) An interaction network of 73 overlap genes was constructed by Cytoscape, larger point means larger degree. (**B**) The top 10 hub genes were identified and displayed a network by MCC algorithm, in which gray value represents the importance in the network.

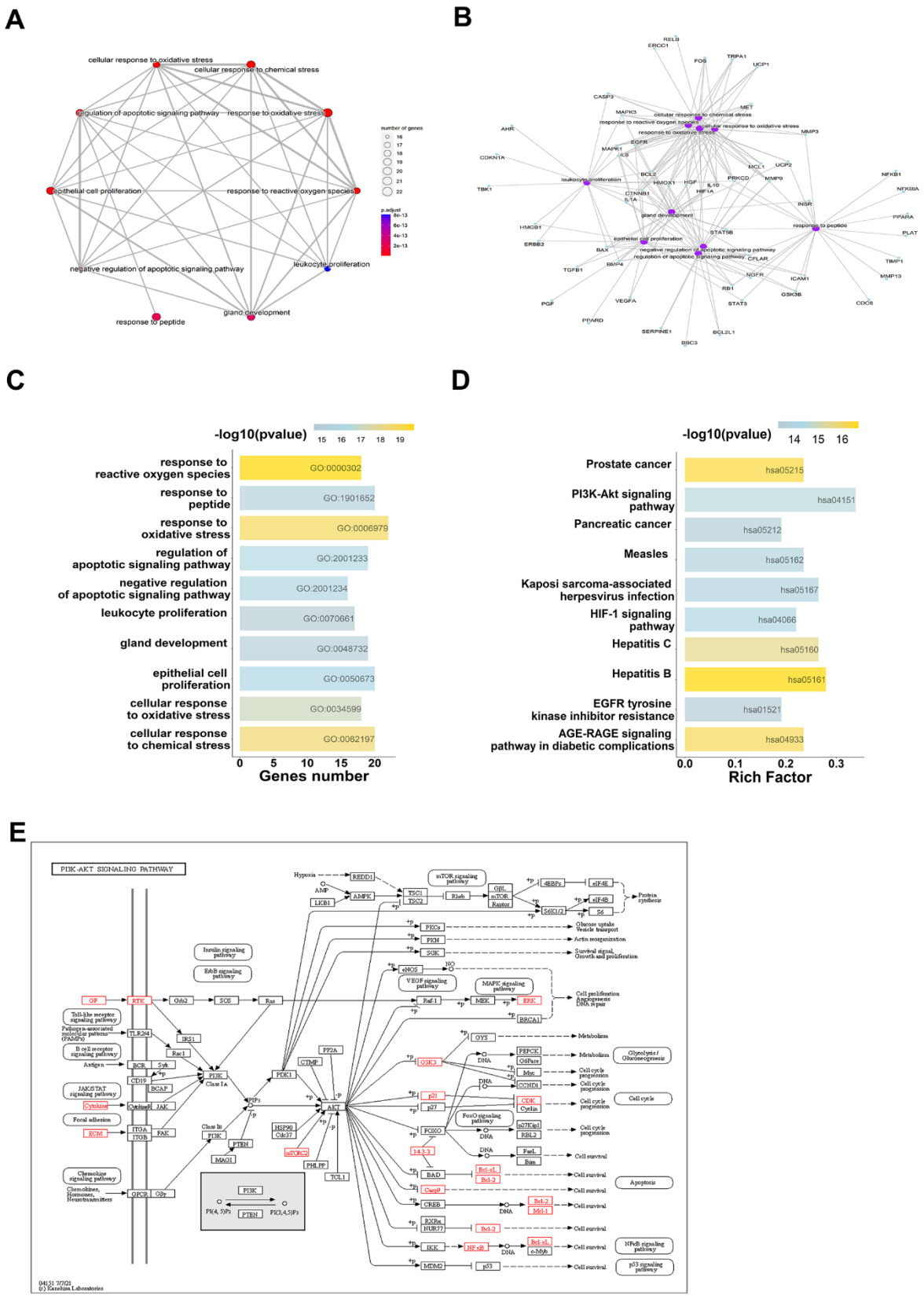

Figure 4. GO and KEGG analysis show the 73 overlap genes targeted by *Atractylodes lancea*. (**A**–**C**) GO enrichment analysis shows the intersection target genes in BP and the top 10 results were displayed. (**D**, **E**) KEGG pathway analysis shows the intersection target genes, top 10 results and the richest factor enrichment pathway - PI3K/AKT signaling pathway were displayed.

Hepatitis C, PI3K/AKT signaling pathway, HIF-1 signaling pathway, Kaposi sarcoma-associated herpesvirus infection (Figure 4D, 4E). Among them, the highest number of intersections genes were enriched in PI3K/AKT signaling pathway. From the enrichment study, *Atractylodes lancea* may exert its anti-cancer activity through PI3K/AKT signaling pathway.

Molecular docking candidate gene screening

To obtain candidate genes for molecular docking, the target genes corresponding to each active ingredient of the drug were intersected with 73 genes, respectively, the component which intersected with the most genes was taken as the core ingredient of the drug. The results indicated that CID:5280445 (luteolin) had the greatest number of intersected genes (Table 1).

Survival, expression, and correlation analysis

To verify the expression of hub-genes in CRC, it was found that MMP3, MMP9, VEGFA, and TIMP1 were significantly differentially expressed in colorectal tumor, compared with normal tissue (Figure 5A–5D). And correlation analysis revealed that all four genes, MMP3, MMP9, VEGFA, and TIMP1, were significantly positively correlated, suggesting that these genes may have synergistic regulatory effects (Figure 5E). The prognostic risk model was constructed using MMP3, MMP9, VEGFA, and TIMP1, and the following formula was obtained: risk score = -0.09264*MMP3 - 0.06919*MMP9 + 0.44883*TIMP1 - 0.04962*VEGFA. In order to evaluate the clinical prognosis of the disease, Kaplan-Meier (KM) and ROC curve analysis was used, and the results showed that the prognostic model composed of MMP3, MMP9, VEGFA, and TIMP1 could effectively predict the prognostic risk of the patients (Figure 5F, 5G).

Molecular docking analysis

To explore whether luteolin, as the core active component of *Atractylodes lancea*, may interact with MMP3, MMP9, VEGFA, and TIMP1, the molecular docking of MMP3, MMP9, VEGFA, and TIMP1 with quercetin was carried out by using Autodock1.5.6 and visualization of docking results by PyMOL. Based on a binding energy of less than -5.0 kcal/mol and the formation of hydrogen bonds between receptor and ligands [32], the molecular docking results were shown in Table 2. The lower the binding energy, the more stable the structure. Among those target genes, MMP3, MMP9, VEGFA, and TIMP1 were found to have the lowest binding energy with luteolin. The 3D interaction between *Atractylodes lancea* and four target genes was shown in Figure 6.

Luteolin represses the malignant phenotypes of CRC cells

To further clarify the effects of luteolin on CRC cells, we performed a series of cellular phenotyping experiments. Before we started, we detected the expression levels of MMP3, MMP9, TIMP1, VEGFA in various colon cancer cell lines by qRT-PCR assay, and found that these genes were highly expressed in RKO and SW480, and we chose RKO and SW480 for the following experiments (Supplementary Figure 2). The cell viability was examined after treatment with different concentrations (0, 20, 40, 80, 160, 200 μM) of luteolin for 48 h by CCK-8 assay. As it was shown in Figure 7A–7D, luteolin inhibited the viability of CRC cells in a dose- and time-dependent manner. Consistent with the results of CCK-8 assays, the anti-proliferation effect of luteolin was confirmed by EdU assay and colony formation experiment (Figure 7E–7G). Wound healing experiments showed that luteolin inhibited cell motility (Figure 7I, 7J). According to the above informatics, qRT-PCR was used to detect the expression of MMP3, MMP9, TIMP1, VEGFA in CRC cells after luteolin treatment, and found that luteolin might down-regulate the expression of MMP3, MMP9, TIMP1, VEGFA in RKO cell lines, and only the expression of MMP3, MMP9 was decreased in SW480 (Figure 7K, 7L). We also found that the protein expression levels of MMP3, MMP9 and the activity of PI3K and AKT were inhibited after luteolin treatment (Figure 7M). In conclusion, luteolin could exert an anti-CRC effect through inhibiting PI3K/AKT signaling pathway.

DISCUSSION

Despite advances in early detection and treatment, the incidence and mortality rates of CRC are still rising [33]. To develop novel prospective therapeutic targets and new drugs, the bioinformatics analysis was used to clarify the prognostic risk factors and targets of CRC. In our study, we predicted the target proteins associated with CRC progression that interacted with *Atractylodes lancea*, and elucidated the relevant mechanisms of anti-CRC effect by integrating information from public databases such as Genecards, GEO, TCGA, TCMSP and so on. Docking studies were performed to predict specific interactions between luteolin which was a core active ingredient of *Atractylodes lancea* and its predicted protein targets.

The overlapped genes shared by CRC and Atractylodes lance were obtained by pharmacology platform, disease database and expression datasets. Finally, 73 genes co-related with *Atractylodes lancea* and CRC and 10 hub genes were identified according to PPI network. The above hub genes were analyzed for GO and KEGG

Table 1. The overlap of each active ingredient targets with 73 genes.

PubChem_ID	Count	Gene
CID:5280445	30	XDH,VRK1,GSTK1,ABCG2,BCL2,CASP9,MMP9,HMOX1,MAPK1,IL6,CASP3,VEGFA,NFKBIA,ERBB2, CDKN1A,CDK2,MCL1,BCL2L1,MET,ICAM1,IL10,INSR,TBK1,ADORA2A,PRKCE,EGFR,HMGB1,PTN, MAPK3,NFKB1
CID:5281703	21	CASP3,HIF1A,CTNNB1,MMP13,NFKB1,PRKCD,BCL2,MCL1,GSK3B,BBC3,CDKN1A,IL6,BAX,CCL26, MMP9,VEGFA,CFLAR,EGFR,SPP1,NEDD4L,MAPK1
CID:445639	14	MMP13,PPARD,PPARA,HMGCR,NTRK2,SERPINE1,CETP,MMP3,UCP2,ERBB2,SOAT1,AQP9,BCL2,STAT5B
CID:10228	12	SMAD1,CASP3,HMGCR,VEGFA,NFKB1,ABCB1,ERCC1,ICAM1,NFKBIA,CTNNB1,IL6,MAPK1
CID:440917	6	ADORA2A,BCL2,CASP3,CASP9,BAX,NFKB1
CID:5281416	6	CASP3,BCL2,CDK2,CDKN1A,RB1,MMP3
CID:985	6	CRTC2,IL10,GUCA2A,BCL2,YWHAZ,IL1A
CID:222284	5	CASP9,CASP3,BCL2,BAX,TGFB1
CID:31404	5	UCP1,HMOX1,BMP4,ICAM1,LBP
CID:5280450	5	PPARA,BCL2,ICAM1,FOS,NFKB1
CID:5321018	3	PGF,IL6,VEGFA
CID:6054	3	PPARA,BAX,STAT3
CID:931	3	FUS,BCL2,UCHL1
CID:31423	2	AHR,UGT1A6
CID:996	2	STAT3,AGTR2
CID:5281515	1	IL6
CID:5281522	1	PPARA
CID:5283349	1	RB1
CID:6989	1	BAX
CID:7410	1	TRPA1
CID:8468	1	HIF1A
CID:91457	1	TRPA1

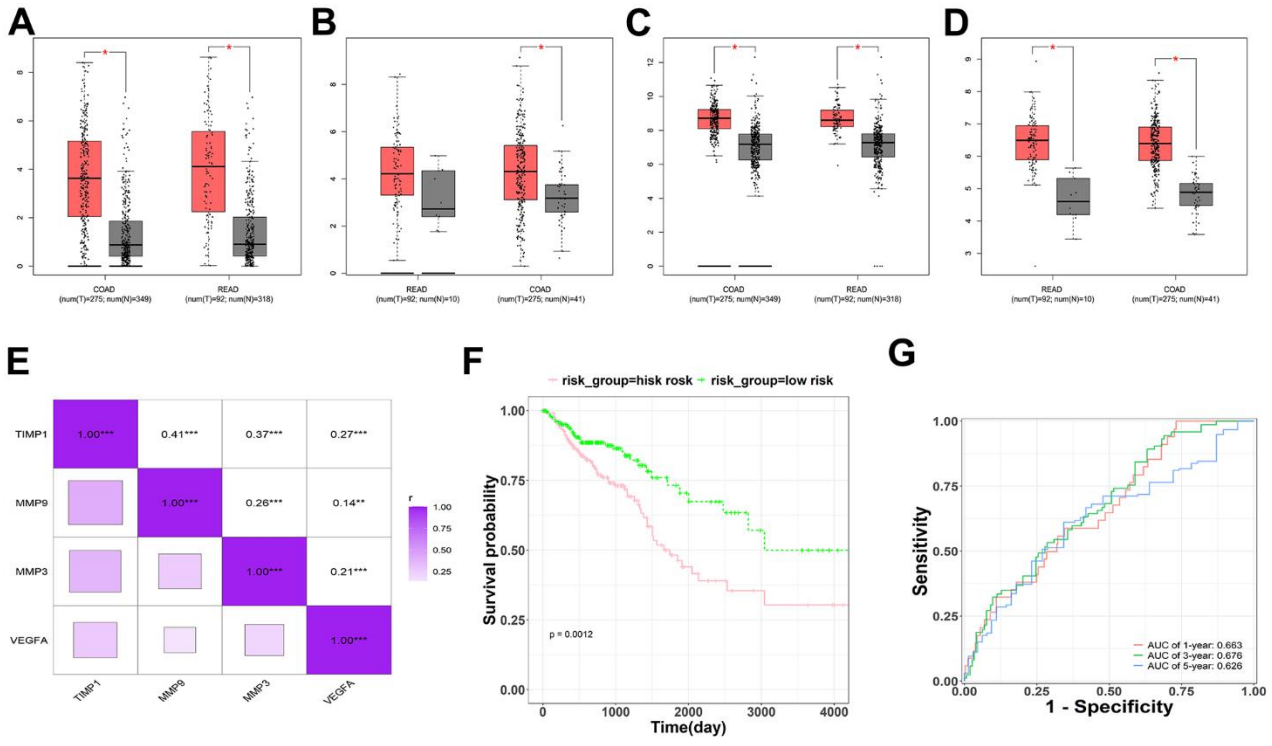

Figure 5. Survival, expression, and correlation analysis of the hub-genes in CRC. (**A**–**D**) Expression analysis for four genes (MMP3, MMP9, TIMP1 and VEGFA), red represents as Tumor, gray represents as Normal. (**E**) The correlation analysis for four genes (MMP3, MMP9, TIMP1 and VEGFA). (**F**) The KM survival plots for prognostic model which consist of four genes (MMP3, MMP9, TIMP1 and VEGFA). (**G**) The ROC curve analysis predicted this prognostic model at 1-, 3-, and 5-year survival rates.

Table 2. The results of molecular docking with luteolin.

Target	PubChem_ID	Compound	Free binding energy (kcal/mol)
MMP3	5280445	Luteolin	-7
MMP9			-10.5
TIMP1			-8.4
VEGFA			-5.9

pathways enrichment. Notably, some of these biological processes analyses identified that *Atractylodes lancea* may act through oxidative stress in response to CRC. And KEGG analysis of *Atractylodes lancea*'s anti-CRC activity revealed several related signaling pathways, including PI3K/AKT signaling pathway, HIF-1 signaling pathway. These signaling pathways are interconnected and known to be associated with oxidative stress [34–36]. Thus, multiple signaling pathways may be involved and contributed to *Atractylodes lancea*'s overall anti-CRC activity.

The molecular docking results of luteolin which as the core ingredients of *Atractylodes lancea* showed that hydrogen bonding was the main forms of interaction. And four genes (MMP3, MMP9, TIMP1 and VEGFA) which have the lowest binding energy to combine with luteolin were found to be involved in CRC progression. Expression analysis showed that MMP3, MMP9, TIMP1 and VEGFA were upregulated in tumor samples. Correlation, survival and ROC curve analysis between those genes supported these results, inferring that MMP3, MMP9 and VEGFA were negatively associated with prognostic risk, and TIMP1 was positively associated with prognostic risk. We inferred that luteolin affects the malignant phenotype of CRC by regulating the expression of MMP3, MMP9, TIMP1 and VEGFA.

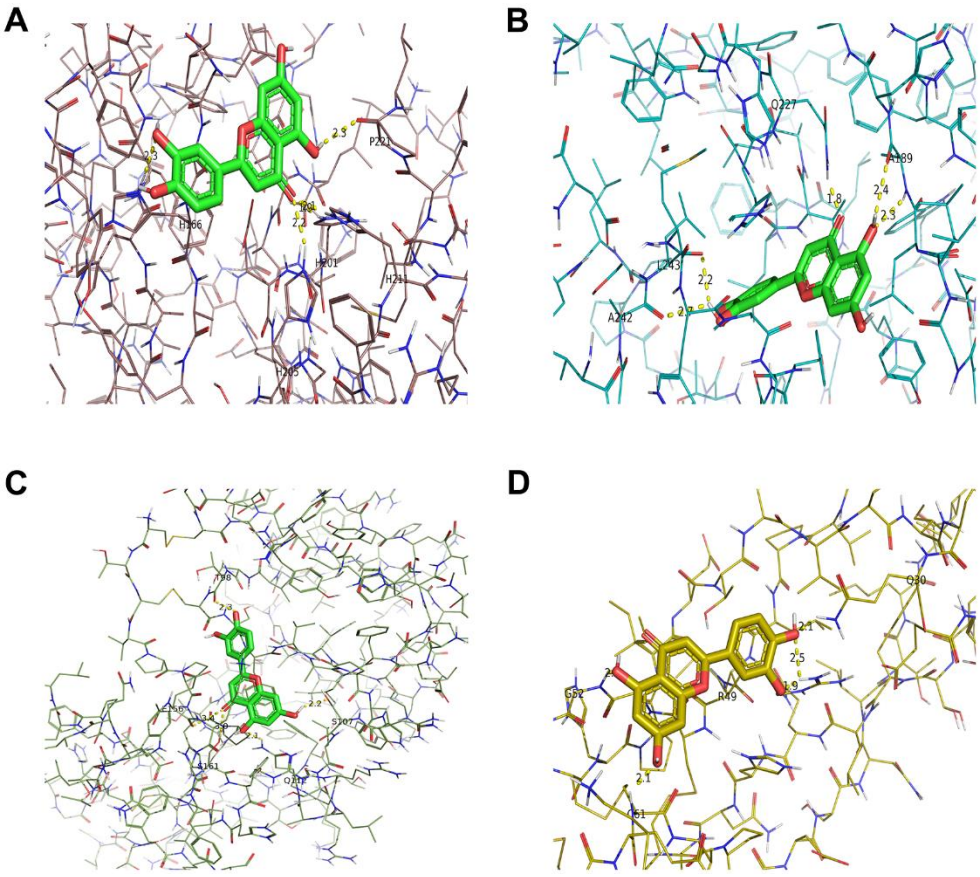

Figure 6. Molecular models of luteolin binding to its predicted protein targets. 3D receptor-ligand interaction diagram for the top four genes with the lowest binding energy for MMP3 (**A**), MMP9 (**B**), TIMP1 (**C**), VEGFA (**D**).

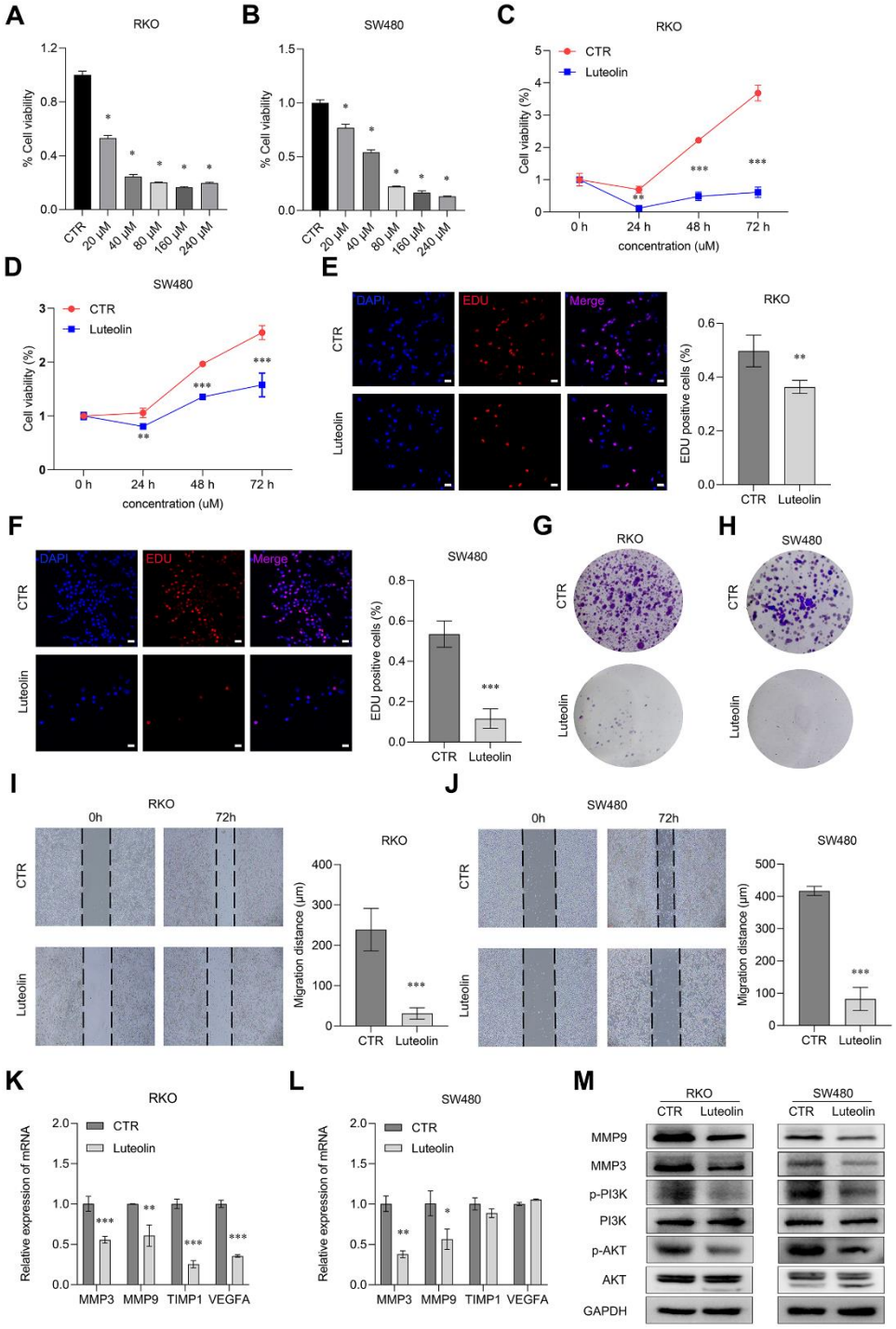

Figure 7. Luteolin represses the malignant phenotypes of CRC cells. (**A**, **B**) After treatment with different concentrations of luteolin (0, 20, 40, 80, 160, 200 μM) for 48 h, the cell viabilities of RKO and SW480 cells were determined by using CCK-8 assay. (**C**, **D**) After treatment with 40 μM luteolin or DMSO (control) for 24 h, 48 h and 72 h, the cell proliferation capacities of RKO and SW480 cells were determined using CCK-8. (**E**, **F**) After treatment with 40 μM luteolin or DMSO (control) for 24 h, the cell proliferation capacities of RKO and SW480 cells were determined using EdU assay. Bar = 20 μm. (**G**, **H**) After treatment with 40 μM luteolin or DMSO (control) for 2 weeks, the cell colonies were stained with crystal violet to display the effect of luteolin on proliferation of RKO and SW480 cells. (**I**, **J**) After treatment with 40 μM luteolin or DMSO (control) for 72 h, the migration distance of RKO and SW480 cells were assayed by wounding healing experiments. (**K**, **L**) After treatment with 40 μM luteolin or DMSO (control) for 24h, the expression level of MMP3, MMP9, TIMP1 and VEGFA in RKO and SW480 cells was detected by qRT-PCR assay. (**M**) After treatment with 40 μM luteolin or DMSO (control) for 24h, the expression levels of MMP9, MMP3, PI3K, p-PI3K, AKT and p-AKT in RKO and SW480 cells was analyzed by Western blot. Data are presented as mean ± SD, * $p < 0.05$, ** $p < 0.01$, *** $p < 0.001$ compared with the control group.

MMPs, which participated to degrade extracellular matrix, plays an important role in CRC metastasis [37]. Degradation of extracellular matrix was essential for tumor invasion and metastasis [38]. Based on using immortalized epithelial cell lines or transgenic mouse models, MMP3 plays an important role in tumor initiation [39]. As well as MMP3, increasing MMP9 transcription enhanced cell invasion [40]. MMP3 and MMP9 expression have been proposed to be a biological predictor in CRC [41]. Previous studies have reported that *Atractylodes lancea* inhibited osteoarthritis by suppressing the expression and activity of MMP3 [42], and *Atractylodes lancea* inhibited migration and invasion of hepatocellular carcinoma cells by decreasing the expression level of MMP9 [43]. Consistent with those studies, we also found that *Atractylodes lancea* suppresses the proliferation of CRC cells, accompanied with a decrease in MMP3 and MMP9 expression.

TIMP1 was expressed at a high level in CRC, and decreased expression level of TIMP1 was significantly associated with poor prognosis of CRC [44]. Down-regulation of TIMP1 inhibited the proliferation and metastasis of colon cancer, but promoted apoptosis through the focal adhesion PI3K/AKT and mitogen-activated protein kinase pathway [45]. High level of TIMP1 was associated with a short overall survival time for CRC patients, especially the plasma level of TIMP1, therefore the expression of TIMP1 could be a potential prognostic indicator [46]. In our research, the expression of TIMP1 in RKO cells was inhibited, but the expression of TIMP1 in SW480 cells has no changes after *Atractylodes lancea* treatment. The reason for this phenomenon may be due to the fact that different tumor cells have different genetic backgrounds.

VEGFA, an endothelial cell-specific mitogen, which participate in physiological and pathological angiogenesis to promote endothelial cell growth, migration, differentiation and vascular permeability [47]. Previous studies have shown that the expression level of VEGF was increased in CRC tissue samples and was associated with poor clinical prognosis [48]. Inhibited VEGFA expression significantly suppressed tumor angiogenesis in CRC cells [49]. VEGFA plays a crucial role in angiogenesis in CRC and has become a major target for anti-angiogenic drugs [50]. It has been reported that codonolactone, a component of *Atractylodes lancea*, was able to inhibit angiogenesis in blast cancer by decreasing the expression level of VEGF [51]. And our results showed that under luteolin treatment, the expression of VEGFA in RKO was decreased. And it could be a candidate for anti-angiogenesis drugs in CRC. The reason for this may be the result in the anti-cancer effects of *Atractylodes lancea* in different cancers with different components.

Many biological activities, including cell proliferation, differentiation, migration, and death, were regulated by PI3K/AKT signaling pathways. Notably, genome-wide association studies have confirmed the PI3K/AKT signaling pathway as one of the genetic markers most closely associated with CRC. In CRC, PI3K/AKT was associated with tumor proliferation, migration, tumor progression and poor prognosis [52]. Our research showed that PI3K/AKT signaling was inhibited under luteolin treatment. A series of studies have been reported that MMP3 [53], MMP9 [54], TIMP1 [45] and VEGFA [55] could be regulated by PI3K/AKT signaling pathway. Therefore, *Atractylodes lancea* inhibited the proliferation and migration of CRC cells by suppressing the expression of MMP3, MMP9, TIMP1 and VEGFA probably through PI3K/AKT signaling pathway.

CONCLUSIONS

Our study analyzed the role, core active component and mechanisms of *Atractylodes lancea* in CRC using network pharmacology and phenotyping experiments. Our findings revealed the anti-CRC effect of *Atractylodes lancea* via an array of targets and pathways. *Atractylodes lancea* may have a therapeutic role in CRC through inhibiting cell proliferation and migration by targeting the hub genes (MMP3, MMP9, TIMP1 and VEGFA) though PI3K/AKT signaling pathway. Despite clarifying the mechanisms of *Atractylodes lancea* with hub genes which need more pre- and clinical experiments, our findings still offer a reference for further investigation of the anti-tumor effect of *Atractylodes lancea* in CRC.

AUTHOR CONTRIBUTIONS

Conceptualization, G.J.Z; Experiments and data collection, G.L.W, C.C.G, H.P, Y.W, K.Y.B; Data analysis, G.L.W, C.C.G, H.P, Y.W, S.Y.L, M.Z, N.W; Writing—original draft preparation, G.L.W, G.J.Z; Project supervision and funding acquisition, G.J.Z. All authors have read and agreed to the published version of the manuscript.

CONFLICTS OF INTEREST

The authors declare that they have no conflict of interest.

FUNDING

This research was supported by the National Natural Science Foundation of China (81870337) and Natural Science Foundation of Guangdong Province (2024A1515012850).

REFERENCES

1. Patel SG, Karlitz JJ, Yen T, Lieu CH, Boland CR. The rising tide of early-onset colorectal cancer: a comprehensive review of epidemiology, clinical features, biology, risk factors, prevention, and early detection. Lancet Gastroenterol Hepatol. 2022; 7:262–74. https://doi.org/10.1016/S2468-1253(21)00426-X PMID:35090605

2. Bürtin F, Mullins CS, Linnebacher M. Mouse models of colorectal cancer: Past, present and future perspectives. World J Gastroenterol. 2020; 26:1394–426. https://doi.org/10.3748/wjg.v26.i13.1394 PMID:32308343

3. Johnson CM, Wei C, Ensor JE, Smolenski DJ, Amos CI, Levin B, Berry DA. Meta-analyses of colorectal cancer risk factors. Cancer Causes Control. 2013; 24:1207–22. https://doi.org/10.1007/s10552-013-0201-5 PMID:23563998

4. McCleary NJ, Meyerhardt JA, Green E, Yothers G, de Gramont A, Van Cutsem E, O'Connell M, Twelves CJ, Saltz LB, Haller DG, Sargent DJ. Impact of age on the efficacy of newer adjuvant therapies in patients with stage II/III colon cancer: findings from the ACCENT database. J Clin Oncol. 2013; 31:2600–6. https://doi.org/10.1200/JCO.2013.49.6638 PMID:23733765

5. Choudhari AS, Mandave PC, Deshpande M, Ranjekar P, Prakash O. Phytochemicals in Cancer Treatment: From Preclinical Studies to Clinical Practice. Front Pharmacol. 2020; 10:1614. https://doi.org/10.3389/fphar.2019.01614 PMID:32116665

6. Koonrungsesomboon N, Na-Bangchang K, Karbwang J. Therapeutic potential and pharmacological activities of Atractylodes lancea (Thunb.) DC. Asian Pac J Trop Med. 2014; 7:421–8. https://doi.org/10.1016/S1995-7645(14)60069-9 PMID:25066389

7. Zhao M, Wang Q, Ouyang Z, Han B, Wang W, Wei Y, Wu Y, Yang B. Selective fraction of Atractylodes lancea (Thunb.) DC. and its growth inhibitory effect on human gastric cancer cells. Cytotechnology. 2014; 66:201–8. https://doi.org/10.1007/s10616-013-9559-1 PMID:23564282

8. Vanaroj P, Chaijaroenkul W, Na-Bangchang K. Atractylodin and β-eudesmol from Atractylodes lancea (Thunb.) DC. Inhibit Cholangiocarcinoma Cell Proliferation by Downregulating the Notch Signaling Pathway. Asian Pac J Cancer Prev. 2023; 24:551–8. https://doi.org/10.31557/APJCP.2023.24.2.551 PMID:36853304

9. Guo W, Liu S, Ju X, Du J, Xu B, Yuan H, Qin F, Li L. The antitumor effect of hinesol, extract from Atractylodes lancea (Thunb.) DC. by proliferation, inhibition, and apoptosis induction via MEK/ERK and NF-κB pathway in non-small cell lung cancer cell lines A549 and NCI-H1299. J Cell Biochem. 2019; 120:18600–7. https://doi.org/10.1002/jcb.28696 PMID:31338882

10. Plengsuriyakarn T, Matsuda N, Karbwang J, Viyanant V, Hirayama K, Na-Bangchang K. Anticancer Activity of Atractylodes lancea (Thunb.) DC in a Hamster Model and Application of PET-CT for Early Detection and Monitoring Progression of Cholangiocarcinoma. Asian Pac J Cancer Prev. 2015; 16:6279–84. https://doi.org/10.7314/apjcp.2015.16.15.6279 PMID:26434829

11. Plengsuriyakarn T, Viyanant V, Eursitthichai V, Picha P, Kupradinun P, Itharat A, Na-Bangchang K. Anticancer activities against cholangiocarcinoma, toxicity and pharmacological activities of Thai medicinal plants in animal models. BMC Complement Altern Med. 2012; 12:23. https://doi.org/10.1186/1472-6882-12-23 PMID:22448640

12. Na-Bangchang K, Kulma I, Plengsuriyakarn T, Tharavanij T, Kotawng K, Chemung A, Muhamad N, Karbwang J. Phase I clinical trial to evaluate the safety and pharmacokinetics of capsule formulation of the standardized extract of Atractylodes lancea. J Tradit Complement Med. 2021; 11:343–55. https://doi.org/10.1016/j.jtcme.2021.02.002 PMID:34195029

13. Plengsuriyakarn T, Kotawong K, Karbwang J, Na-Bangchang K. Preclinical studies of toxicity and anti-cholangiocarcinoma activity of the standardized capsule formulation of Atractylodes lancea (Thunb.) DC. BMC Complement Med Ther. 2023; 23:186. https://doi.org/10.1186/s12906-023-03992-z PMID:37287012

14. Chen MH, May BH, Zhou IW, Zhang AL, Xue CC. Integrative Medicine for Relief of Nausea and Vomiting in the Treatment of Colorectal Cancer Using Oxaliplatin-Based Chemotherapy: A Systematic Review and Meta-Analysis. Phytother Res. 2016; 30:741–53. https://doi.org/10.1002/ptr.5586 PMID:26912094

15. Chen M, May BH, Zhou IW, Sze DM, Xue CC, Zhang AL. Oxaliplatin-based chemotherapy combined with traditional medicines for neutropenia in colorectal cancer: A meta-analysis of the contributions of specific plants. Crit Rev Oncol Hematol. 2016; 105:18–34. https://doi.org/10.1016/j.critrevonc.2016.07.002 PMID:27497028

16. Zong S, Tang Y, Li W, Han S, Shi Q, Ruan X, Hou F. A Chinese Herbal Formula Suppresses Colorectal Cancer

Migration and Vasculogenic Mimicry Through ROS/HIF-1 α/MMP2 Pathway in Hypoxic Microenvironment. Front Pharmacol. 2020; 11:705. https://doi.org/10.3389/fphar.2020.00705 PMID:32499699

17. Chen M, May BH, Zhou IW, Xue CC, Zhang AL. FOLFOX 4 combined with herbal medicine for advanced colorectal cancer: a systematic review. Phytother Res. 2014; 28:976–91. https://doi.org/10.1002/ptr.5092 PMID:24343974

18. Lin H, Wang X, Wang L, Dong H, Huang P, Cai Q, Mo Y, Huang F, Jiang Z. Identified the Synergistic Mechanism of Drynariae Rhizoma for Treating Fracture Based on Network Pharmacology. Evid Based Complement Alternat Med. 2019; 2019:7342635. https://doi.org/10.1155/2019/7342635 PMID:31781279

19. Wang XW, Zhang CA, Ye M. Study on the Mechanism of Xiaotan Sanjie Recipe in the Treatment of Colon Cancer Based on Network Pharmacology. Biomed Res Int. 2022; 2022:9498109. https://doi.org/10.1155/2022/9498109 PMID:36033553

20. Yan D, Zheng G, Wang C, Chen Z, Mao T, Gao J, Yan Y, Chen X, Ji X, Yu J, Mo S, Wen H, Han W, et al. HIT 2.0: an enhanced platform for Herbal Ingredients' Targets. Nucleic Acids Res. 2022; 50:D1238–43. https://doi.org/10.1093/nar/gkab1011 PMID:34986599

21. Ru J, Li P, Wang J, Zhou W, Li B, Huang C, Li P, Guo Z, Tao W, Yang Y, Xu X, Li Y, Wang Y, Yang L. TCMSP: a database of systems pharmacology for drug discovery from herbal medicines. J Cheminform. 2014; 6:13. https://doi.org/10.1186/1758-2946-6-13 PMID:24735618

22. Huang L, Xie D, Yu Y, Liu H, Shi Y, Shi T, Wen C. TCMID 2.0: a comprehensive resource for TCM. Nucleic Acids Res. 2018; 46:D1117–20. https://doi.org/10.1093/nar/gkx1028 PMID:29106634

23. Safran M, Dalah I, Alexander J, Rosen N, Iny Stein T, Shmoish M, Nativ N, Bahir I, Doniger T, Krug H, Sirota-Madi A, Olender T, Golan Y, et al. GeneCards Version 3: the human gene integrator. Database (Oxford). 2010; 2010:baq020. https://doi.org/10.1093/database/baq020 PMID:20689021

24. Amberger JS, Hamosh A. Searching Online Mendelian Inheritance in Man (OMIM): A Knowledgebase of Human Genes and Genetic Phenotypes. Curr Protoc Bioinformatics. 2017; 58:1.2.1–1.2.12. https://doi.org/10.1002/cpbi.27 PMID:28654725

25. Kim J, So S, Lee HJ, Park JC, Kim JJ, Lee H. DigSee: Disease gene search engine with evidence sentences (version cancer). Nucleic Acids Res. 2013; 41:W510–7. https://doi.org/10.1093/nar/gkt531 PMID:23761452

26. Ritchie ME, Phipson B, Wu D, Hu Y, Law CW, Shi W, Smyth GK. limma powers differential expression analyses for RNA-sequencing and microarray studies. Nucleic Acids Res. 2015; 43:e47. https://doi.org/10.1093/nar/gkv007 PMID:25605792

27. Chen H, Boutros PC. VennDiagram: a package for the generation of highly-customizable Venn and Euler diagrams in R. BMC Bioinformatics. 2011; 12:35. https://doi.org/10.1186/1471-2105-12-35 PMID:21269502

28. Szklarczyk D, Gable AL, Nastou KC, Lyon D, Kirsch R, Pyysalo S, Doncheva NT, Legeay M, Fang T, Bork P, Jensen LJ, von Mering C. The STRING database in 2021: customizable protein-protein networks, and functional characterization of user-uploaded gene/measurement sets. Nucleic Acids Res. 2021; 49:D605–12. https://doi.org/10.1093/nar/gkaa1074 PMID:33237311 Erratum in: Nucleic Acids Res. 2021; 49:10800. https://doi.org/10.1093/nar/gkab835 PMID:34530444

29. Yu G, Wang LG, Han Y, He QY. clusterProfiler: an R package for comparing biological themes among gene clusters. OMICS. 2012; 16:284–7. https://doi.org/10.1089/omi.2011.0118 PMID:22455463

30. Bahmani A, Tanzadehpanah H, Hosseinpour Moghadam N, Saidijam M. Introducing a pyrazolopyrimidine as a multi-tyrosine kinase inhibitor, using multi-QSAR and docking methods. Mol Divers. 2021; 25:949–65. https://doi.org/10.1007/s11030-020-10080-8 PMID:32297121

31. Seeliger D, de Groot BL. Ligand docking and binding site analysis with PyMOL and Autodock/Vina. J Comput Aided Mol Des. 2010; 24:417–22. https://doi.org/10.1007/s10822-010-9352-6 PMID:20401516

32. Feng C, Zhao M, Jiang L, Hu Z, Fan X. Mechanism of Modified Danggui Sini Decoction for Knee Osteoarthritis Based on Network Pharmacology and Molecular Docking. Evid Based Complement Alternat Med. 2021; 2021:6680637. https://doi.org/10.1155/2021/6680637 PMID:33628311

33. Zhang R, Zhao J, Xu J, Jiao DX, Wang J, Gong ZQ, Jia JH. Andrographolide suppresses proliferation of human colon cancer SW620 cells through the TLR4/NF-κB/MMP-9 signaling pathway. Oncol Lett. 2017; 14:4305–10.

https://doi.org/10.3892/ol.2017.6669 PMID:28943944

34. Mazurakova A, Koklesova L, Csizmár SH, Samec M, Brockmueller A, Šudomová M, Biringer K, Kudela E, Pec M, Samuel SM, Kassayova M, Hassan STS, Smejkal K, et al. Significance of flavonoids targeting PI3K/Akt/HIF-1α signaling pathway in therapy-resistant cancer cells - A potential contribution to the predictive, preventive, and personalized medicine. J Adv Res. 2024; 55:103–18. https://doi.org/10.1016/j.jare.2023.02.015 PMID:36871616

35. Shiau JP, Chuang YT, Cheng YB, Tang JY, Hou MF, Yen CY, Chang HW. Impacts of Oxidative Stress and PI3K/AKT/mTOR on Metabolism and the Future Direction of Investigating Fucoidan-Modulated Metabolism. Antioxidants (Basel). 2022; 11:911. https://doi.org/10.3390/antiox11050911 PMID:35624775

36. Hayes JD, Dinkova-Kostova AT, Tew KD. Oxidative Stress in Cancer. Cancer Cell. 2020; 38:167–97. https://doi.org/10.1016/j.ccell.2020.06.001 PMID:32649885

37. Pezeshkian Z, Nobili S, Peyravian N, Shojaee B, Nazari H, Soleimani H, Asadzadeh-Aghdaei H, Ashrafian Bonab M, Nazemalhosseini-Mojarad E, Mini E. Insights into the Role of Matrix Metalloproteinases in Precancerous Conditions and in Colorectal Cancer. Cancers (Basel). 2021; 13:6226. https://doi.org/10.3390/cancers13246226 PMID:34944846

38. Najafi M, Farhood B, Mortezaee K. Extracellular matrix (ECM) stiffness and degradation as cancer drivers. J Cell Biochem. 2019; 120:2782–90. https://doi.org/10.1002/jcb.27681 PMID:30321449

39. Radisky DC, Levy DD, Littlepage LE, Liu H, Nelson CM, Fata JE, Leake D, Godden EL, Albertson DG, Nieto MA, Werb Z, Bissell MJ. Rac1b and reactive oxygen species mediate MMP-3-induced EMT and genomic instability. Nature. 2005; 436:123–7. https://doi.org/10.1038/nature03688 PMID:16001073

40. Loesch M, Zhi HY, Hou SW, Qi XM, Li RS, Basir Z, Iftner T, Cuenda A, Chen G. p38gamma MAPK cooperates with c-Jun in trans-activating matrix metalloproteinase 9. J Biol Chem. 2010; 285:15149–58. https://doi.org/10.1074/jbc.M110.105429 PMID:20231272

41. Zeng C, Chen Y. HTR1D, TIMP1, SERPINE1, MMP3 and CNR2 affect the survival of patients with colon adenocarcinoma. Oncol Lett. 2019; 18:2448–54. https://doi.org/10.3892/ol.2019.10545 PMID:31452735

42. Moon PD, Jeong HS, Chun CS, Kim HM. Baekjeolyusin-tang and its active component berberine block the release of collagen and proteoglycan from IL-1β-stimulated rabbit cartilage and down-regulate matrix metalloproteinases in rabbit chondrocytes. Phytother Res. 2011; 25:844–50. https://doi.org/10.1002/ptr.3353 PMID:21089182

43. Cheng Y, Chen T, Yang X, Xue J, Chen J. Atractylon induces apoptosis and suppresses metastasis in hepatic cancer cells and inhibits growth *in vivo*. Cancer Manag Res. 2019; 11:5883–94. https://doi.org/10.2147/CMAR.S194795 PMID:31388314

44. Łukaszewicz-Zając M, Mroczko B. Circulating Biomarkers of Colorectal Cancer (CRC)-Their Utility in Diagnosis and Prognosis. J Clin Med. 2021; 10:2391. https://doi.org/10.3390/jcm10112391 PMID:34071492

45. Song G, Xu S, Zhang H, Wang Y, Xiao C, Jiang T, Wu L, Zhang T, Sun X, Zhong L, Zhou C, Wang Z, Peng Z, et al. TIMP1 is a prognostic marker for the progression and metastasis of colon cancer through FAK-PI3K/AKT and MAPK pathway. J Exp Clin Cancer Res. 2016; 35:148. https://doi.org/10.1186/s13046-016-0427-7 PMID:27644693

46. Yukawa N, Yoshikawa T, Akaike M, Sugimasa Y, Rino Y, Masuda M, Imada T. Impact of plasma tissue inhibitor of matrix metalloproteinase-1 on long-term survival in patients with colorectal cancer. Oncology. 2007; 72:205–8. https://doi.org/10.1159/000112827 PMID:18160809

47. Dakowicz D, Zajkowska M, Mroczko B. Relationship between VEGF Family Members, Their Receptors and Cell Death in the Neoplastic Transformation of Colorectal Cancer. Int J Mol Sci. 2022; 23:3375. https://doi.org/10.3390/ijms23063375 PMID:35328794

48. Ellis LM, Takahashi Y, Liu W, Shaheen RM. Vascular endothelial growth factor in human colon cancer: biology and therapeutic implications. Oncologist. 2000. https://doi.org/10.1634/theoncologist.5-suppl_1-11 PMID:10804085

49. Hu F, Sun X, Li G, Wu Q, Chen Y, Yang X, Luo X, Hu J, Wang G. Inhibition of SIRT2 limits tumour angiogenesis via inactivation of the STAT3/VEGFA signalling pathway. Cell Death Dis. 2018; 10:9. https://doi.org/10.1038/s41419-018-1260-z PMID:30584257

50. Jayson GC, Kerbel R, Ellis LM, Harris AL. Antiangiogenic therapy in oncology: current status and future directions. Lancet. 2016; 388:518–29. https://doi.org/10.1016/S0140-6736(15)01088-0 PMID:26853587

51. Wang S, Cai R, Ma J, Liu T, Ke X, Lu H, Fu J. The natural compound codonolactone impairs tumor induced angiogenesis by downregulating BMP signaling in endothelial cells. Phytomedicine. 2015; 22:1017–26. https://doi.org/10.1016/j.phymed.2015.07.009 PMID:26407944

52. Stefani C, Miricescu D, Stanescu-Spinu II, Nica RI, Greabu M, Totan AR, Jinga M. Growth Factors, PI3K/AKT/mTOR and MAPK Signaling Pathways in Colorectal Cancer Pathogenesis: Where Are We Now? Int J Mol Sci. 2021; 22:10260. https://doi.org/10.3390/ijms221910260 PMID:34638601

53. Gao XW, Su XT, Lu ZH, Ou J. 17β-Estradiol Prevents Extracellular Matrix Degradation by Downregulating MMP3 Expression via PI3K/Akt/FOXO3 Pathway. Spine (Phila Pa 1976). 2020; 45:292–9. https://doi.org/10.1097/BRS.0000000000003263 PMID:31809475

54. Hao H, Wang B, Yang L, Sang Y, Xu W, Liu W, Zhang L, Jiang D. miRNA-186-5p inhibits migration, invasion and proliferation of breast cancer cells by targeting SBEM. Aging (Albany NY). 2023; 15:6993–7007. https://doi.org/10.18632/aging.204887 PMID:37477531

55. Zhu F, Zheng J, Xu F, Xi Y, Chen J, Xu X. Resveratrol Alleviates Dextran Sulfate Sodium-Induced Acute Ulcerative Colitis in Mice by Mediating PI3K/Akt/VEGFA Pathway. Front Pharmacol. 2021; 12:693982. https://doi.org/10.3389/fphar.2021.693982 PMID:34497510

SUPPLEMENTARY MATERIALS

Supplementary Figures

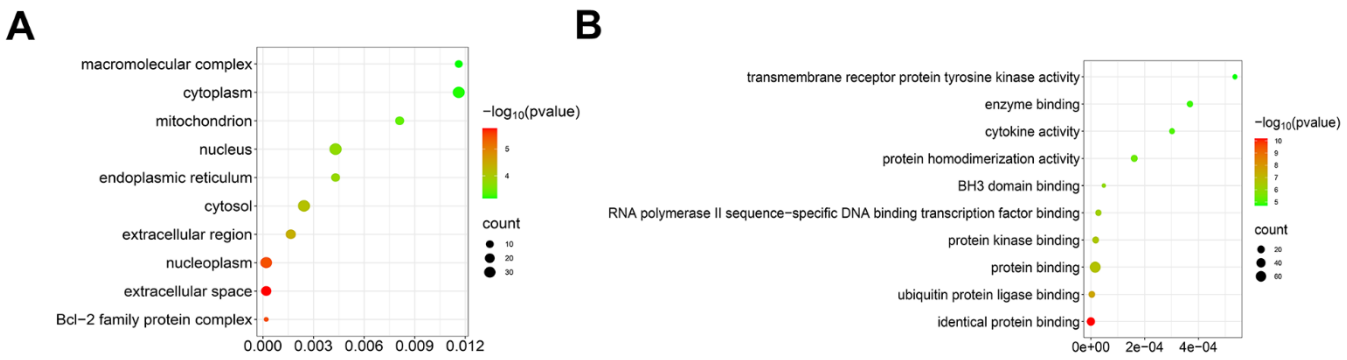

Supplementary Figure 1. GO enrichment analysis shows the cellular components and molecular function of 73 overlapping genes. (**A**) GO enrichment analysis shows the intersection target genes in cellular components localization and the top 10 results were displayed. (**B**) GO enrichment analysis shows the intersection target genes in molecular function localization and the top 10 results were displayed.

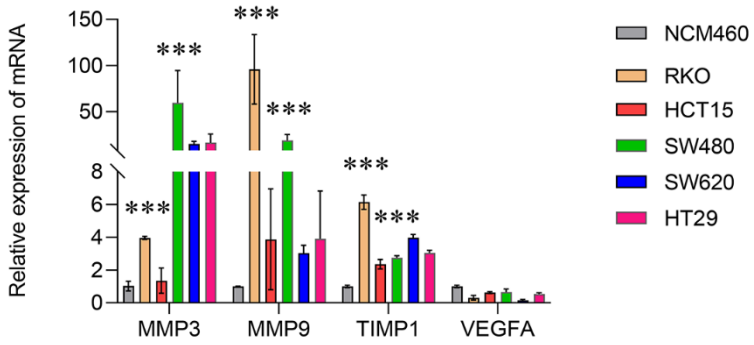

Supplementary Figure 2. The expression levels of MMP3, MMP9, TIMP1 and VEGFA in CRC cell lines were detected by qRT-PCR.

Supplementary Tables

Please browse Full Text version to see the data of Supplementary Tables 3–6, 8, 9.

Supplementary Table 1. Sequence information for primers used in qRT-PCR.

Gene	Forward sequence	Reverse sequence
18S	5'-AACCCGTTGAACCCCATT -3'	5'-CCATCCAATCGGTAGTAGCG -3'
MMP3	5'- CGGTTCCGCCTGTCTCAAG-3'	5'- CGCCAAAAGTGCCTGTCTT-3'
MMP9	5'- GGGACGCAGACATCGTCATC-3'	5'- TCGTCATCGTCGAAATGGGC-3'
TIMP1	5'- AGAGTGTCTGCGGATACTTCC-3'	5'- CCAACAGTGTAGGTCTTGGTG-3'
VEGFA	5'- AGGGCAGAATCATCACGAAGT-3'	5'- AGGGTCTCGATTGGATGGCA-3'

Supplementary Table 2. The active ingredients of *Atractylodes lancea*.

PubChem_ID	Cpd_name
CID:10228	Osthole
CID:6989	Thymol
CID:8468	Vanillic Acid
CID:5281703	Wogonin
CID:931	Naphthalene
CID:996	Phenol
CID:985	Palmitic Acid
CID:1140	Toluene
CID:7095	Biphenyl
CID:7410	Acetophenone
CID:31423	Pyrene
CID:31404	Butylated Hydroxytoluene
CID:445639	Oleic Acid
CID:222284	Beta-Sitosterol
CID:853433	Isoeugenol
CID:5280445	Luteolin
CID:5280450	Linoleic Acid
CID:5281416	Esculetin
CID:6054	Phenylethyl Alcohol
CID:440917	D-Limonene
CID:227829	Guaiol
CID:5281522	Isocaryophyllene
CID:91457	beta-Eudesmol
CID:5283349	2,4-Decadienal
CID:5281520	Alpha-Humulone
CID:5281515	Caryophyllene
CID:7044	Decahydronaphthalene
CID:7461	gamma-Terpinene
CID:31272	Butyl acetate
CID:60961	Adenosine
CID:10878761	Hinesol
CID:675	5,6-Dimethylbenzimidazole
CID:676946	p-Coumaric acid ethyl ester
CID:7362	Furfural

CID:460	Guaiacol
CID:6885	Phthalide
CID:5280794	Stigmasterol
CID:5541	Triacetin
CID:5281426	Umbelliferone
CID:5283345	2-Decenal
CID:442353	beta-Chamigrene
CID:5283316	2-Heptenal
CID:5283356	2-Undecenal
CID:3080635	Atractylon
CID:5321047	Atractylodin
CID:10012964	Atractylodinol
CID:10929902	Atractyloside I
CID:71448957	Atractyloside G
CID:71307451	Atractyloside A
CID:12366272	Cirsiumaldehyde
CID:14079045	Icariside F2
CID:71448952	Atractyloside B
CID:71448953	Atractyloside C
CID:71448954	Atractyloside D
CID:71448955	Atractyloside E
CID:12138536	α-Hexylcinnamaldehyde
CID:10353528	Agarospirol
CID:1549992	Bisabolol
CID:71448961	3beta-Hydroxyatractylon
CID:78249	Limonene
CID:5317844	alpha-Guaiene
CID:3084961	Wogonoside
CID:5321018	Atractylenolide I
CID:14420566	Parthenolide
CID:70697841	Gaillardin
CID:12309818	beta-Eudesmol cis epimer
CID:5356634	Stigmastenone
CID:6429301	(Z)-caryophyllene
CID:92138	Elemol
CID:14448070	Atractylenolide II
CID:13986099	3,5-Bis(tert-butyl) benzaldehyde
CID:6451614	Stigmastanol

Supplementary Table 3. Predicted targets of the potential bioactive compounds of *Atractylodes lancea*.

Supplementary Table 4. Relevant targets for colorectal cancer disease.

Supplementary Table 5. Differentially expression genes of colorectal cancer in GSE164191 datasets.

Supplementary Table 6. Differentially expression genes of colorectal cancer in TCGA.

Supplementary Table 7. Predicted targets of the potential bioactive compounds of *Atractylodes lancea* (73 genes).

geneName	source	uniprot
CTNNB1	DigSee	P35222
BCL2L1	DigSee	Q07817
STAT3	DigSee	P40763
EGFR	DigSee	P00533
BCL2	DigSee	P10415
HIF1A	DigSee	Q16665
MMP9	DigSee	P14780
VEGFA	DigSee	P15692
NFKB1	DigSee	P19838
SERPINE1	DigSee	P05121
IL10	DigSee	P22301
ABCB1	DigSee	P08183
CDKN1A	DigSee	P38936
MCL1	DigSee	Q07820
GSK3B	DigSee	P49841
BAX	DigSee	Q07812
UCHL1	DigSee	P09936
MET	DigSee	P08581
ERBB2	DigSee	P04626
CDK2	DigSee	P24941
XDH	DigSee	P47989
PPARA	DigSee	Q07869
PPARD	DigSee	Q03181
IL6	DigSee	P05231
SPP1	DigSee	P10451
TGFB1	DigSee	P01137
ERCC1	DigSee	P07992
NFKBIA	DigSee	P25963
PGF	DigSee	P49763
HMOX1	DigSee	P09601
HMGB1	DigSee	P09429
BMP4	DigSee	P12644
ICAM1	DigSee	P05362
MAPK3	DigSee	P27361
FOS	DigSee	P01100
MAPK1	DigSee	P28482
INSR	DigSee	P06213
FUS	DigSee	P35637
CASP3	DigSee	P42574
ABCG2	DigSee	Q9UNQ0
MMP3	DigSee	P08254
GUCA2A	DigSee	Q02747
GSTK1	DigSee	Q9Y2Q3
NTRK2	DigSee	Q16620
RB1	DigSee	P06400
CFLAR	DigSee	O15519

CASP9	DigSee	P55211
HMGCR	DigSee	P04035
IL1A	DigSee	P01583
AHR	DigSee	P35869
SOAT1	DigSee	P35610
UCP2	DigSee	P55851
PTN	DigSee	P21246
BBC3	OMIM	Q9BXH1
UGT1A6	GeneCards	P19224
MMP13	GeneCards	P45452
TBK1	GeneCards	Q9UHD2
LBP	GeneCards	P18428
AGTR2	GeneCards	P50052
PRKCE	GeneCards	Q02156
UCP1	GeneCards	P25874
CCL26	GeneCards	Q9Y258
PRKCD	GeneCards	Q05655
NEDD4L	GeneCards	Q96PU5
SMAD1	GeneCards	Q15797
YWHAZ	GeneCards	P63104
STAT5B	GeneCards	P51692
AQP9	GeneCards	O43315
CETP	GeneCards	P11597
CRTC2	GeneCards	Q53ET0
ADORA2A	GeneCards	P29274
TRPA1	GeneCards	O75762
VRK1	GeneCards	Q99986

Supplementary Table 8. GO enrichment analysis of potential target genes of *Atractylodes lancea*'s potential bioactive compounds (p-value < 0.05).

Supplementary Table 9. KEGG pathways enrichment analysis of potential target genes of *Atractylodes lancea*'s potential bioactive compounds (p-value ≤ 0.05).